Properties of Poly(urea-formaldheyde) Microcapsules Containing an Epoxy Resin

S. Cosco,[1] V. Ambrogi,[1] P. Musto,[2] C. Carfagna[1,2]

[1]*Department of Materials and Production Engineering, University of Naples ''Federico II'', P.le Tecchio, 80-80125 Napoli, Italy*
[2]*Institute of Chemistry and Technology of Polymers (ICTP), CNR, c/o Comprensorio Olivetti, Via Campi Flegrei, Pozzuoli, Napoli, Italy*

Received 21 March 2006; accepted 24 July 2006
DOI 10.1002/app.26263
Published online 23 April 2007 in Wiley InterScience (www.interscience.wiley.com).

ABSTRACT: Physical properties of urea-formaldehyde microcapsules containing an epoxy resin are presented and discussed. Microcapsules were prepared by *in situ* polymerization of monomers in an oil-in-water emulsion. Differential scanning calorimetry, thermogravimetric analysis, and scanning electronic microscopy were applied to investigate thermal and morphological microcapsule properties. Microencapsulation was detected by means of FTIR and Raman techniques. It was found that the amount of encapsulated epoxy resin as well as the extent of urea-formaldehyde polymerization depends on the reaction temperature and the stirring speed. © 2007 Wiley Periodicals, Inc. J Appl Polym Sci 105: 1400–1411, 2007

Key words: microencapsulation; emulsion polymerization; infrared spectroscopy; resins; Raman spectroscopy

INTRODUCTION

Microencapsulation is a process by which small particles or droplets are surrounded by a coating to produce capsules in the micrometer to millimeter range known as microcapsules.[1–3] The material inside the capsule is refereed to as the core, internal phase or fill, whereas the wall is sometimes called a shell, coating or membrane.

The first industrial product employing microencapsulation was carbonless copy paper developed by Green and Schleicher in the 1950s. The microcapsules used in it were prepared by complex coacervation of gelatin and gum arabic.[4] Carbonless copy paper is one of the most significant products to utilize microencapsulation technology, and it is still produced commercially. The technologies employed for carbonless copy paper have led to the development of various microcapsule products in recent years.

Microcapsules have found application in a number of fields ranging from chemicals[5,6] and pharmaceuticals[7,8] to cosmetics[9,10] and printing[11] and a widespread interest has developed in microencapsulation technology.

Summarizing, depending on the application envisioned and on the materials and methods used to prepare them, the microcapsules may have a diameter ranging from about 10–250 μm and a multitude of different shapes and structures ranging from simple droplets of liquid core material surrounded by a spherical shell, to irregularly-shaped particles containing small droplets of core material dispersed in a continuous polymer shell matrix.

There are numerous basic microencapsulation techniques employed to produce this wide range of structures and many of these have several variations. More detailed features of microcapsules are summarized in books by Gutcho[12] and Arshady,[13] and in review articles by Makino,[14] Arshady,[15] Kondo,[16] Hatate et al.,[17] and Yoshizawa and Hatate.[18–20]

Microcapsules can encapsulate various substances, such as gases, liquids, and solids, to form composite materials on a scale of millimetres. Coating substances can be selected from a wide variety of natural or synthetic polymers, depending on the material to be coated and the characteristics desired in the final microcapsules. The coating composition is one of the key parameter affecting the functional properties of the microcapsule.

Because almost no coating material can meet all the requirements, in practice they are used in combination with other coating materials and/or modifiers.

These core-shell microcapsules exhibit significant promise for providing new ''smart'' functionality for applications related to the general field of intelligent microstructures and microsystems,[21–25] and for applications in the phase change materials (PCM's)[26] as well as in the self healing composites.[27] These composites autonomically heal cracks as they develop in a structure. When a crack forms it ruptures embedded microcapsules that release a healing agent. The agent flows into the crack through capillary action and is

Correspondence to: S. Cosco (cosco@na.infn.it).

Journal of Applied Polymer Science, Vol. 105, 1400–1411 (2007)

polymerized by a catalyst in the matrix of the composite.

To obtain a self-repairing composite the polymeric matrix has to contain a self-repair system that does not affect the material's overall properties or performance. It must also be able to sense damage, and then be able to react to that damage and initiate healing. Finally, it must restore the material's original properties (strength and stiffness, for example).

This article reports on the preparation and characterization of urea-formaldehyde (UF) microcapsules containing an epoxy resin to be used as fillers in self-healing materials.

The wall material has to avoid leakage and diffusion of the encapsulated agent for considerable time. Moreover, when used as fillers for composites, a high bond strength to the host polymer combined with a moderate strength microcapsule shell are required to remain intact during processing of the polymeric matrix. For this purpose a urea-formaldheyde based material was selected. UF resins are the most important type of the so-called aminoplastic resins that consist of linear or branched oligomeric and polymeric molecules, which also always contain some amount of monomer.[28] After hardening UF resins form an insoluble, three-dimensional network and cannot be melted or thermoformed again.

Epoxy resin was chosen as the encapsulated agent of interest thanks to its extreme versatility, as it has found use in many advanced fields, ranging from electrical/electronic to aircraft/aerospace and automotive industries.[29]

Factors determining the microencapsulability of the core material were described. In particular, our interest was devoted to a better understanding of the influence of the reaction parameters on the microcapsule properties.

To evaluate the relation between the experimental conditions and the encapsulability a set of urea-formaldehyde microcapsules containing an epoxy resin was prepared by *in situ* polymerization in an oil-in-water emulsion, in which reaction time and temperature and stirring speed were modulated.

Scanning electronic microscopy (SEM) was performed to investigate on microcapsule size and surface morphology. TGA, DSC, Raman and FT-IR analyses were carried out with the aim of evaluate the thermal stability of the microcapsules, the extent of microencapsulation and the shell features.

Infrared and Raman spectroscopy are complementary tools for obtaining vibrational spectra. Depending on the nature of the vibration, which is determined by the symmetry of the molecule, vibrations may be active or forbidden in the infrared or Raman spectrum. Infrared active are all vibrations which modulate the molecular dipole moment. Raman active are vibrations which modulate the molecular polarizability. Based on the different selection rules of these two spectroscopic techniques, polar bonds tend to yield strong IR and weak Raman bands, whereas nonpolar groups give rise to strong Raman and weak IR bands.[30] Further advantages of Raman compared to mid infrared are the lack of interferences from water vapor and glass, which is very convenient because glass sample containers can be used during experiments.

EXPERIMENTAL

Materials

Urea (supplied from Fluka), formaldehyde 37 wt % solution in water, ammonium chloride and resorcinol (purchased from Aldrich Milan, Italy) were used for the preparation of microcapsules.

Ethylene maleic anhydride (EMA) copolymer was used as emulsifier and purchased from Aldrich Milan, Italy. As the encapsulated agent, a commercial available Bisphenol-F-type epoxy resin (PY306) was selected and supplied by Huntsman/Vantico (Italy).

All these products were used without further purification.

Preparation of microcapsules

Formation of urea-formaldehyde microcapsules was achieved by *in situ* polymerization in an oil-in-water emulsion. In a typical procedure 2.5 g urea, 0.25 g ammonium chloride and 0.25 g resorcinol were dissolved in water (150 mL), under magnetic stirring and at room temperature.

Since in some cases it may be desirable to use an emulsion stabilizer, a 2.5 wt % aqueous solution of EMA copolymer (50 mL) was added to the reaction mixture. The emulsion stabilizers has the function to form thin layer around the capsule core entities and thereby to stabilize the emulsion. The pH was adjusted to 3.5 using sodium hydroxide (NaOH) and hydrochloric acid (HCl). Thirty milliliter of PY306 were added to the solution to form an emulsion and allowed to stabilize for 10 min. 6.3 g of 37 wt % aqueous solution of formaldehyde were added to the emulsion to obtain a 1 : 1.9 *M* ratio of formaldehyde to urea. The temperature was raised to the selected value.

After a fixed time of reaction under continuous stirring, the mixer and hot plate were switched off. Once cooled to room temperature, the suspension of microcapsules was separated under vacuum filtration and then washed with chloroform to eliminate the residual (non encapsulated) epoxy resin. The microcapsules were isolated by filtration and vacuum dried at 40°C for 24 h.

Instrumental

Scanning electronic microscopy (SEM) was used to study the morphology of microcapsules, using a Leica Cambridge Stereoscan microscope model 440. Prior to being observed, samples were metallized with a gold layer.

To confirm the microencapsulation process as well as to get a semiquantitative evaluation of amount of microencapsulated epoxy resin DSC analysis was carried out.

A TA Instruments model 2920 calorimeter was used to detect on thermal behavior of microcapsules core and shell. For each sample, a single scan from 0 to 300°C at a heating rate of 10°C/min, under nitrogen atmosphere, was carried out.

The thermal stability of the microcapsules was investigates by using a thermogravimetric analyzer (Dupont model 951). For each sample a simple scan was performed at a heating rate of 10°C/min from room temperature up to 600°C under N_2 flow.

FTIR spectra of microsphere samples were obtained in transmission mode using a System 2000 spectrometer from Perkin–Elmer (Norwalk, CT). This instrument employs a germanium/KBr beam splitter and a deuterated tryglycine sulfate (DTGS) detector. The instrumental parameters adopted for the spectral collection were as follows: resolution 4 cm^{-1}, optical path difference (OPD) velocity = 0.20 cm s^{-1}, and spectral range 4000–400 cm^{-1} resulting in 3551 collected data points.

To exactly evaluate the amount of epoxy resin encapsulated Raman spectroscopy was used. Raman spectra were collected on a Nicolet Nexus NIR FT-Raman spectrometer from Thermo Nicolet (Madison, WI, USA), equipped with a diode pumped Nd-YAG laser ($\lambda = 1064$ nm) as an excitation source operating at 0.85–1.05 W of power, and a room temperature InGaAs photoelectric detector. The backscattered radiation was collected at 180° to the laser beam direction. Typical spectra were recorded in the range 3800–200 cm^{-1}, at a resolution of 4 cm^{-1}, coadding 500 scans to improve the signal-to-noise ratio. The specimens, in the form of finely ground powders were sampled in glass vials. Raman spectroscopy was used for the quantitative evaluation of the encapsulated epoxy resin.

To separate the individual peaks in the case of unresolved, multicomponent bands, a curve resolving algorithm was employed, based on the Levenberg-Marquardt method.[31] To reduce the number of adjustable parameters and to ensure the uniqueness of the result, the band shape and the number of components were fixed. The number of components and their initial positions were estimated by looking at the negative peaks of the second-derivative spectra. To account for the fluorescence effect the baseline was simulated by a third-order polynomial function. The program was allowed to calculate, by a nonlinear curve fitting of the data, the height, the full width at half height (FWHH) and the position of the individual components. The peak function used throughout was a mixed Gauss-Lorentz line shape.[32]

RESULTS AND DISCUSSION

Urea-formaldehyde microcapsules were synthesized as described in the *Experimental part*. In particular, five different samples were prepared varying the experimental conditions, such as reaction time and temperature and stirring rate, as summarized in Table I.

Neat urea-formaldehyde was also prepared in the same condition of sample A.

Chemical reaction in urea-formaldehyde resins

The synthesis of UF resins from urea and formaldehyde is basically a two step process[26,33]: the first is the so-called methylolation reaction, which is catalyzed by both acids and bases and leads to the formation of hydroxymethyl compounds (monomethylol, dimethylol and trimethylolurea). Methylolation refers to the addition of up to three molecules of the bifunctional formaldehyde to one molecule of urea. It is known that tetramethylolurea has never been isolated.[34] The formation of methylol groups mostly depends on the F/U molar ratio, with higher molar ratio increasing the tendency to form highly methylolated species.[35,36] Molar ratio lower than $\sim$ 1.8 lead to some precipitation during the following acid condensation step, causing inhomogenities in the solution.

In a second step, the condensation reaction between the various methylol species and urea takes place. This reaction is mainly acid catalyzed and leads to a complex mixture of low molecular weight UF oligomers. The condensing moieties link together by methylene ($N—CH_2—N$) or by dimethylene ether ($—N—CH_2—O—CH_2—N—$) groups. At low pH, the as produced UF resins cure irreversibly to form a crosslinked network. This reaction can be induced by

TABLE I
Reaction Parameters (Temperature, Time, and Stirring Rate) Selected for the Preparation of Urea-Formaldheyde Microcapsules

Sample	Reaction temperature (°C)	Reaction time (h)	Stirring rate (rpm)
Neat UF	60	4	2000
A	60	4	2000
B	60	6	2000
C	40	4	2000
D			1600
E			1200

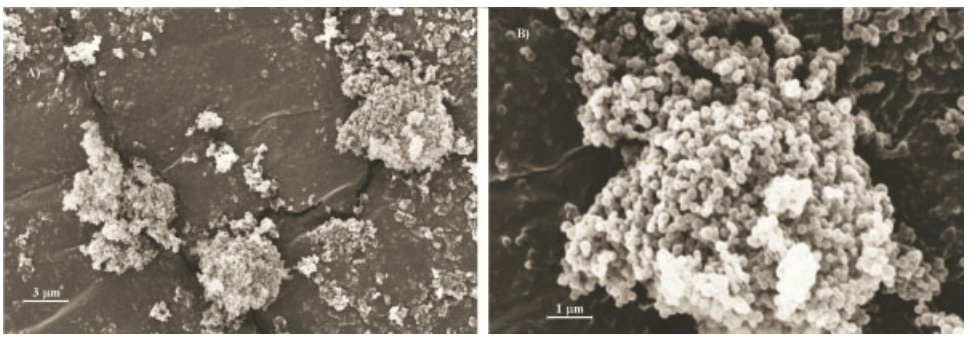

Figure 1 SEM micrographs of pure urea-formaldheyde at (A) 10K× and (B) 30K× magnification.

addition of catalyst or hardeners (ammonium chloride and ammonium sulfate) and/or of further branchers, such as resorcinol, involved in the cocondensation reaction with urea and formaldehyde.[37,38] The incorporation or resorcinol improves the low resistance of UF bonds to the influence of water. Moreover, it proceeds quickly upon heating resulting in the formation of tridimensional networks and ultimately a thermosetting resin that is no longer thermoformable.

Microcapsule morphology

To examinate the morphological features of synthesized microcapsules SEM analysis was carried out, as reported in the micrographs of Figures 1–4.

All the samples exhibit a complex morphology, characterized by micro-sized beads with a partially rough outer surface (single oil droplets), and/or clusters of nanocapsules. Irregularly shaped capsules (termed as *aggregates*) were also observed, in which the core material was subdivided into a number of parts embedded in a continuum of wall material.

Encapsulation proceeds via liquid-liquid phase separation. Polymerization between urea and formaldehyde is initiated in the water phase where a low molecular weight prepolymer forms. As the molecular size increases, the polymer deposits at the organic-aqueous interface, in which the organic phase is constituted by the epoxy monomer.[39] The polymerization continues to give a highly crosslinked urea-formaldehyde capsule wall in the presence of resorcinol and ammonium chloride. The formation of urea-formaldehyde nanoparticles is attributed to precipitation of higher molecular weight prepolymer in the aqueous solution and their agglomeration and deposition on the capsule surface.

The sample morphology is further complicated by the development of a wide variety of structures in the UF prepolymers which are undoubtedly present after the cure, as reported above.

According to the mechanism proposed above for the case of a sample composed by pure UF [Fig. 1(A,B)] clusters of nanocapsules formed by precipitation of the cured, high-molecular weight portions was found. No evidence of micro-sized particles was detected. In this case, the reaction between urea and formaldehyde occurred exclusively in the aqueous phase, since the epoxy-based droplets, acting as a substrate for the interfacial polymerization, were absent.

As far as the microcapsules containing the epoxy resin concerns, a different and more complex morphology is evident in SEM micrographs. Figure 2 shows the SEM images of sample A which is very similar to that observed for the samples B and C, differing on the reaction time and temperature used for their preparation respectively (Table I). The microcap-

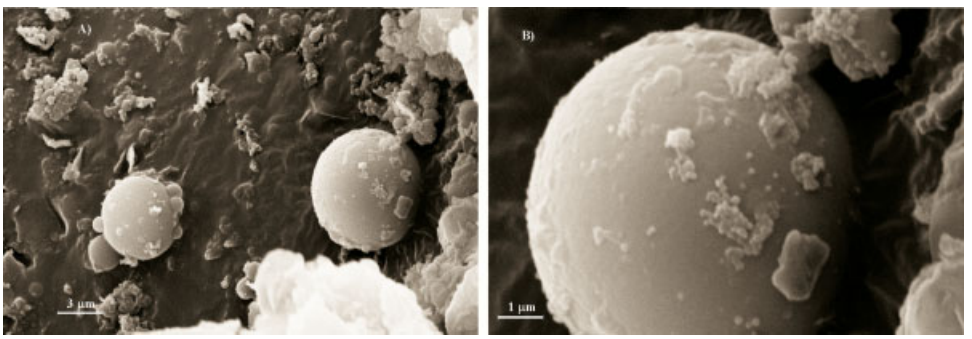

Figure 2 SEM micrographs of sample A at (A) 10K× and (B) 30K× magnification.

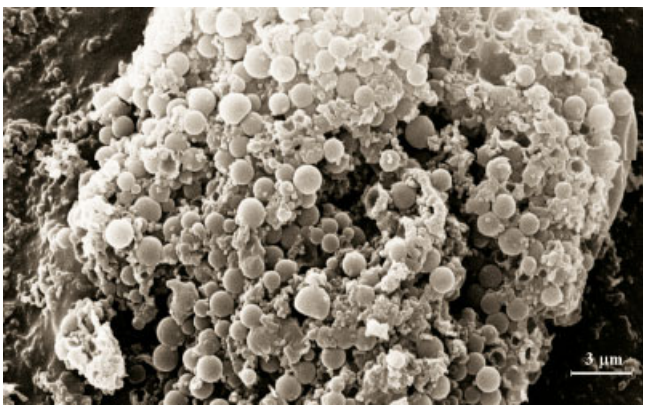

Figure 3 SEM micrographs of sample D at 30K× magnification.

sule diameters are in the range between 5 and 15 μm in the three cases. The morphology of sample A, as well as of samples B and C, is characterized by the presence of microcapsules, *aggregates* and agglomerates of nanoparticles.

Samples D and E were obtained using a reaction temperature $T = 40^{\circ}C$ and two different stirring rates (Table I). Their morphology was very similar to that observed for the sample composed by pure UF and it was characterized by a widespread amount of agglomerated nanosized particles (Figs. 3 and 4). Most probably, in both cases, because of the lower reaction temperature and stirring rate, the organic phase was not well dispersed in the aqueous medium and the urea-formaldehyde system reacted predominantly in the water phase.

Thermal analysis

To investigate on the presence of the epoxy resin into the capsules, a thermal analysis by DSC was carried out. The collected data provided also information about the extent of polymerization of the UF walls. The results are summarized in Table II.

The DSC curves of the prepared samples are reported in Figure 5 in comparison with the thermogram of hollow UF capsules with the aim to evaluate the effect of the reaction temperature on the encapsulating capability. For this purpose, the peak centered at $T = 225^{\circ}C$ was taken into account, since it was not possible to refer to the melting point of the epoxy resin as a diagnostic peak indicating the achievement of the encapsulation. In fact, once the epoxy resin was melted to be added to the reaction solution, it was not able to recrystallize, retaining its viscous state for a long time.

The peak at $T = 225^{\circ}C$ is likely to be attributed to the homopolymerization of the epoxy monomer. It is known that epoxies are reactive towards self-polymerization to polyethers at high temperatures ($T = 200^{\circ}C$) and in the presence of impurities, such acidic and basic compounds.[40,41] These species most probably were captured into the capsules during the wall formation.

Since the ΔH associated to the homopolymerization reaction is unchanged for sample A and B, that differ to each other only on the reaction time used for their preparation (Table I), it can be asserted that the reaction time does not affect the epoxy resin encapsulability.

On the other hand, the ΔH associated to the homopolymerization reaction is higher for sample A ($\Delta H = 390$ J/g) with respect to the sample C ($\Delta H = 330$ J/g), indicating a superior amount of encapsulated resin in the first case. This can be explained in terms of a more efficient dispersion of the core agent with increasing the temperature in the case of sample A. In fact, at $T = 60^{\circ}C$ the epoxy resin is above its melting point and its reduced viscosity favors the homogeneous emulsification throughout the aqueous phase. Moreover, at this temperature the urea-formaldehyde system is more reactive, leading to a complete polymerization within the fixed reaction time ($t = 4$ h). This was also confirmed by the absence of the two broad endothermic peaks centered at $T = 127^{\circ}C$ and $T = 228^{\circ}C$ respectively, associated to the unreacted formaldehyde, urea, and UF oligomers.

The same peaks are easily detectable in the case of neat UF and in the samples D and E.

As far as the neat UF concerns, although the reaction temperature was set at $T = 60^{\circ}C$ it seems that the polymerization did not reach the completion. This could be ascribed to the absence of the epoxy resin droplets, which somehow act as seeding sites for the UF polymerization.

Finally, the peak diagnostic for the epoxy resin appears weak in the curve of sample D, whereas it is not detectable in the thermogram in the case of sample E, analogously to hollow UF particles. Most probably, because of the lower stirring rate, the epoxy

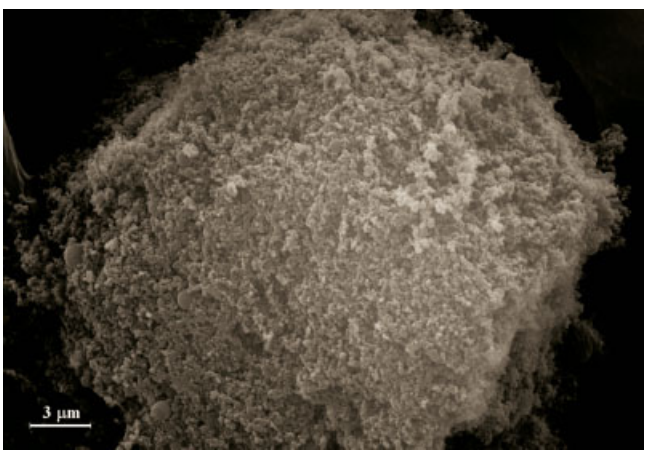

Figure 4 SEM micrographs of sample E at 30K× magnification.

TABLE II
ΔH and Temperature Values Associated to the Epoxy Resin Homopolymerization in the Microcapsules

Sample	$T_{rection}$ (°C)	$t_{reaction}$ (h)	Stirring rate (rpm)	$\Delta H_{homopol}$ (J/g)	$T_{homopol}$ (°C)
Neat UF	60	4	2000	–	–
A	60	4	2000	390	223
B	60	6	2000	391	228
C	40	4	2000	330	229
D	40	4	1600	101	200
E	40	4	1200	13	212

resin/water interfacial surface was reduced and the UF polymerization occurred predominantly in the water phase.

From these results it can assumed that both the temperature and the stirring rate affect the extent of polymerization of the UF wall. Low reaction temperature and stirring rate force the monomer to react in the aqueous rather than at the epoxy/water interface, leading not only to different chemical urea-formaldehyde derivatives but also to a decreased encapsulation capability.

Vibrational analysis (FTIR and Raman spectroscopies)

The FTIR spectrum of the pure urea-formaldehyde resin in the 4000–400 cm^{-1} range is reported in Figure 6.

A broad absorption centered at around 3379 cm^{-1} is likely related to a considerable amount of absorbed water, with possible contributions from the stretching vibrations of residual amine groups. Prominent spectral features are observed at 1630–1559 cm^{-1}, corresponding, respectively, to the amide I mode (mostly C=O stretching) and the amide II mode (prevailingly *N*-CO stretching). A well defined shoulder is detected at higher wavenumbers (1710 cm^{-1}). The complex profile observed in the carbonyl region reflects the multiplicity of molecular structures formed upon curing.

The FTIR spectrum of the neat epoxy resin (Fig. 6) is richer and considerably more resolved. Residual hydroxyl groups, formed during the synthesis, together with absorbed H_2O, produce the broad band centered at 3512 cm^{-1}; the CH_2/CH stretching modes give rise to the complex multiplet in the 3100–2800 cm^{-1} region. The *p*-substituted aromatic rings produce intense absorptions at 1610, 1585, 1509, 1178, 840, and 756 cm^{-1}; the highly coupled C—O—C stretching modes absorb at 1298 and 1242 cm^{-1}. The epoxy ring gives rise to a well resolved peak at 916 cm^{-1} (ring deformation) and to a second peak at around 860 cm^{-1}, partly superimposed onto an aromatic absorption band. The spectra of the investigated microcapsules, in the form of powders dispersed in KBr, are reported in Figure 6. Spectra of samples A and B are dominated by the contribution of the epoxy resin, although the UF skin is readily detectable both in the ν_{OH} and in the carbonyl region. Spectrum of sample C is intermediate; spectra of samples D and E closely resemble the spectrum of the neat UF resin, but some of the more intense peaks of the epoxy component (i.e., at 1509 and 1452 cm^{-1}) are still readily detectable.

From the powder spectra of Figure 6 it is possible to isolate the epoxy resin spectrum by subtracting out the contribution of the UF resin. The results of such analysis, relative to sample B, is displayed in Figure 7. The difference spectrum obtained in this way is essentially coincident with that of the neat epoxy resin (compare Figs. 6 and 7), apart from the sloping base-line from 4000 to 1800 cm^{-1} in spectrum of sample C, because of the scattering of solid microcapsules having the same size of the incident IR radiation (2.5–5.5 μm). This effect is not observed in the spectrum of the neat epoxy resin, which is liquid at room temperature. The ratio between the absorbance of a peak characteristic of the epoxy ring, i.e., at 916 cm^{-1}, (A_{916}) over that of a peak expected to be invariant under the condition used to prepare the samples (typically a well resolved aromatic absorption like the one at 756 cm^{-1}, A_{756}) is proportional to the concentration of

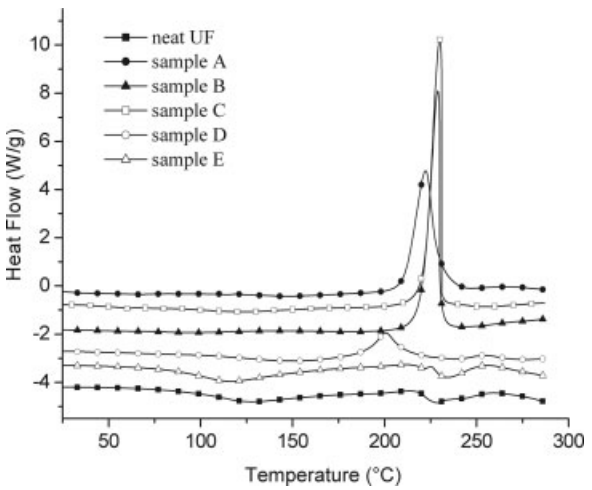

Figure 5 DSC thermograms of prepared microcapsules.

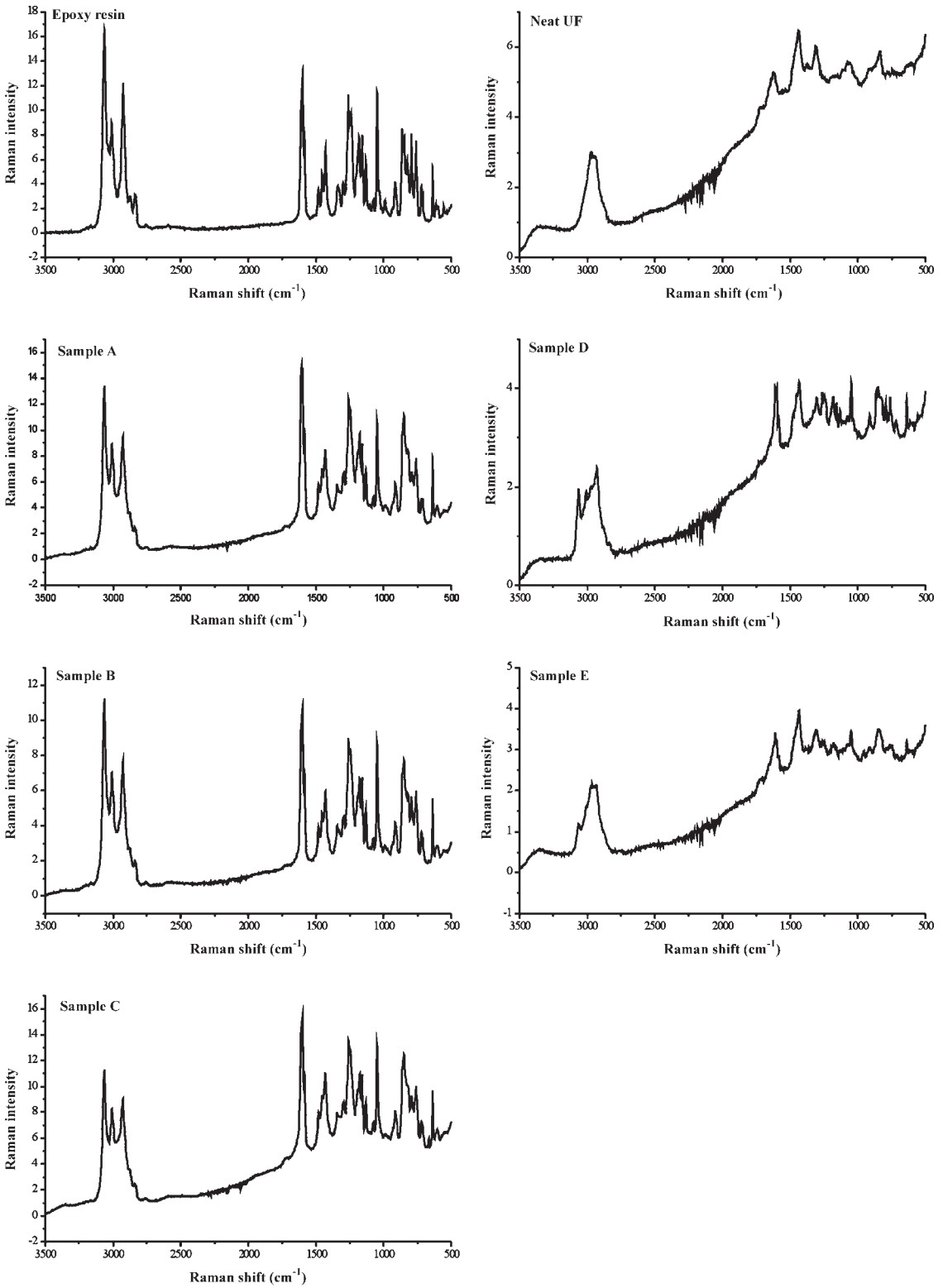

Figure 6 FTIR spectra of prepared microcapsules.

epoxy groups. This ratio is equal to 0.63 ± 0.025 for samples A and C, 0.64 ± 0.025 for sample B and 0.63 ± 0.025 for the pure epoxy resin. Samples D and E, gave unreliable difference spectra because of the very low amount of epoxy resin incorporated in the microcapsules. The analysis demonstrates that no side reactions leading to the consumption of epoxy groups take place in the conditions used to prepare the microcapsules. In terms of the relative ratio of the two components in the microcapsules, the FTIR data qual-

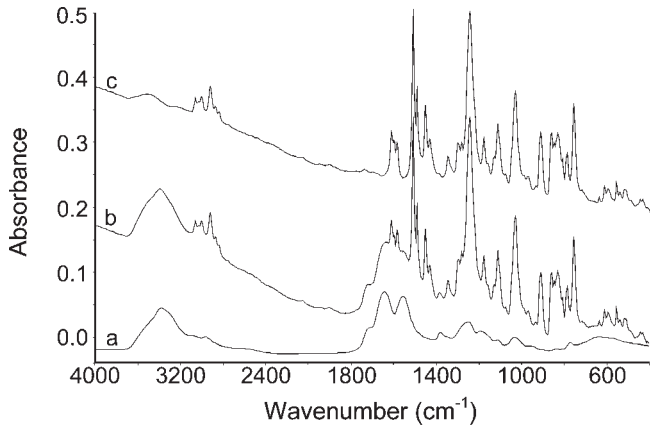

Figure 7 FT-IR spectra of (A) urea-formaldheyde resin, (B) sample B and (C) difference spectrum between sample B and urea-formaldheyde resin.

itatively indicate that encapsulation has been successfully achieved for samples A and B, for which the amount of epoxy resin considerably exceeds that of the surrounding UF skin. Sample C displays a roughly one-to-one ratio between the two components, whereas for sample D and even more so for sample E, the encapsulation procedure is to be considered inefficient. However, difficulties related to the estimation of the total sample content and to the achievement of a perfectly homogeneous dispersion, limit the usefulness of KBr powder spectra in providing reliable quantitative data (uncertainities ≥10%). For a more precise analysis of the samples composition we turned our attention to Raman spectroscopy.

The Raman spectra of the microcapsules prepared in the present study are reported in Figure 8, along with the spectra of the pure components for comparison.

The epoxy resin gives rise to an intense Raman scattering, in the 4000–400 cm^{-1} range, thus producing an essentially noise-free spectrum. As generally found, the Raman peaks are considerably sharper than their infrared counterparts, thus providing a more resolved spectrum. The ν_{CH} region displays fully resolved components at 3063 cm^{-1} (ν Ar-H), 3008 cm^{-1} (ν CH epoxy), 2925 (ν_{asym} CH_2 ether) 2873 (ν_{sym} Ar—(CH_2—(Ar) and 2836 cm^{-1} (ν_{sym} CH_2 ether). Of particular relevance for the present investigation is a well resolved triplet with maxima at 1609, 1600, and 1587 cm^{-1}, assigned to ring stretching modes of the disubstituted aromatics. The epoxy group gives rise to several characteristic peaks at 1263, 1132, 917, and 864 cm^{-1}. The UF resin produces a much lower amount of Raman scattering with respect to the epoxy, and a correspondingly worse spectrum, characterized by intense fluorescence, as indicated by the steep slope of the baseline. In spite of the low intensity and the poor signal-to-noise ratio, several peaks can be identified and assigned. A broad band in the region 3050–2800 cm^{-1} originates from the methylene groups, whereas the amide carbonyls produce an unresolved multiplet with maxima at 1716 and 1623 cm^{-1}. Again, the multicomponent profile in the carbonyl stretching region is a consequence of the complexity of the resin structure.[41,42]

Two bands at 1470 (shoulder) and 1438 cm^{-1} are assigned, respectively, to the bending mode of methylene units in the $N—CH_2—N$ and in the $CH_2—OH$ structures.[41,43]

The spectra of samples A, B and C are very similar to the spectrum of the epoxy resin. However, the fluorescence increases in going from sample A to sample C, which reflects the growing contribution of the UF phase to the overall scattering process. Spectra of samples D and E closely resemble the spectrum of the UF resin, thus indicating that in these two cases the UF component is largely predominant. As for the FTIR spectra, however, also in these cases the more intense peaks of the epoxy resin, notably those in the 1660–1560 cm^{-1} range, remain clearly detectable.

Raman spectroscopy is well established as a quantitative analytical technique. In fact, by assuming a direct proportionality between the normalized intensity of a characteristic Raman peak and the concentration of the scattering species, we may write:

$$\frac{I_{UF}}{I_{EPO}} = \frac{I_{1722}}{I_{1585}} = k\frac{C_{UF}}{C_{EPO}} \quad (1)$$

from which

$$\left(\frac{C_{EPO}}{C_{UF}}\right)_S = \left(\frac{I_{1722}}{I_{1585}}\right)_{STD} \times \left(\frac{I_{1585}}{I_{1722}}\right)_S \times \left(\frac{C_{EPO}}{C_{UF}}\right)_{STD} \quad (2)$$

where I_{1722} and I_{1585} are the intensities of two peaks characteristic, respectively, of the UF and the epoxy resins and C_{EPO} and C_{UF} refer to their concentration, expressed in weight %. The subscripts *S* and *STD* indicate, respectively, the sample being analyzed and a standard mixture of known composition prepared by mechanical mixing of the two resins.

Because of severe peak overlapping in the region of interest, a curve fitting analysis was performed to evaluate I_{1722} and I_{1585}. The results are displayed in Figure 9 for the UF resin, for the epoxy resin and for a representative microcapsule sample (sample C). In all cases the correspondence between the simulated and the experimental profiles is excellent and the peak parameters, i.e., the full width at half height (FWHH), the position and the band-shape, as evaluated from the spectra of the pure resins closely correspond to those obtained for the composite spectra. This confirms the reliability of the method. The percentage of epoxy resin over the total sample weight, as evaluated from eq. (2) for all the investigated specimens is reported in Table III.

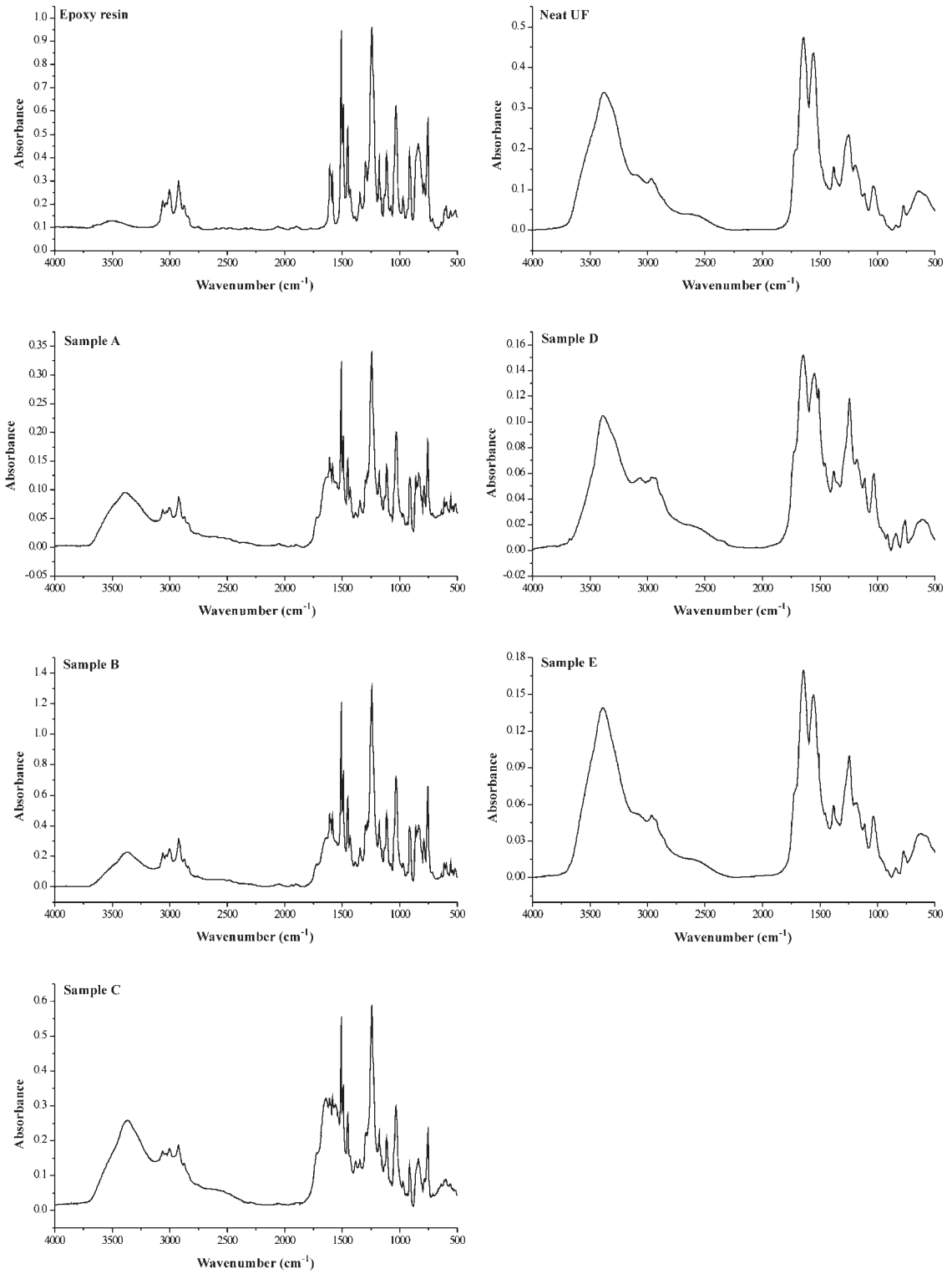

Figure 8 Raman spectra of prepared microcapsules.

TGA analysis

Figure 10 shows the weight loss percentage for a representative set of microcapsules (samples A, C and E) with respect to that of neat UF and of epoxy resin, as a function of temperature. The collected data are summarized in Table IV.

The thermograms of the samples A, C and E exhibit two weight loss steps. To analyze each degradation step the curves of neat UF and epoxy resin were taken into account.

The most significant weight loss (62 wt %) of neat UF occurs in a range between 150 and 300°C, while

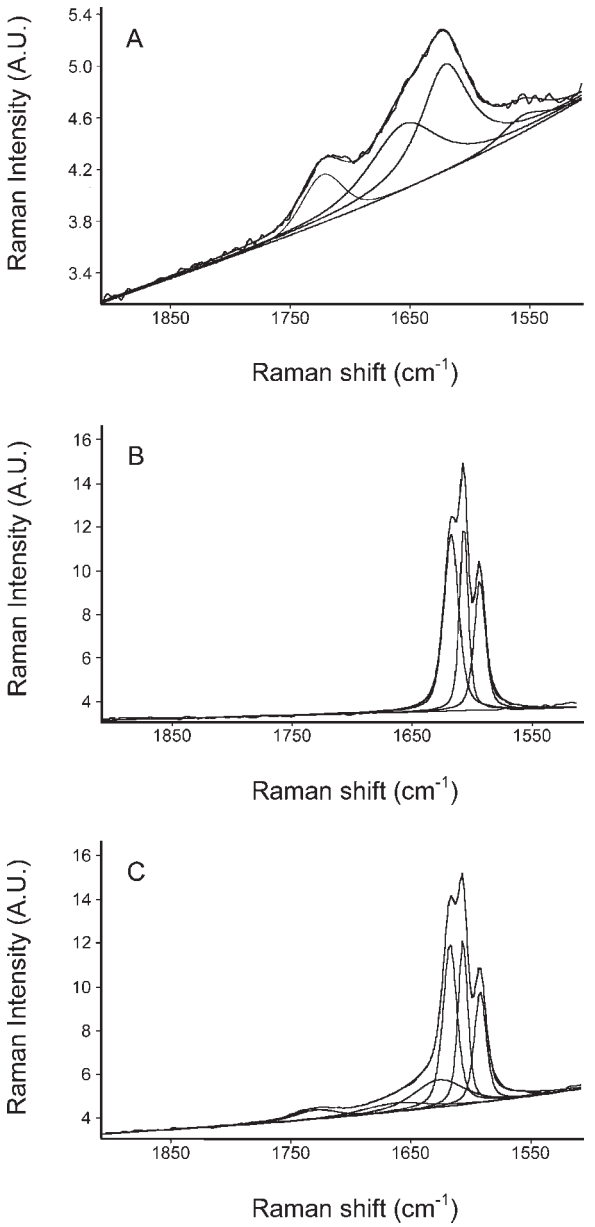

Figure 9 Fittings curves of Raman spectra of (A) urea-formaldheyde resin, (B) epoxy resin and (C) sample C.

the epoxy resin thermal decomposition starts at $T = 225^{\circ}C$, to reach the 50 wt % loss at $T_d = 322^{\circ}C$.

If we analyze the curve of sample A, in the temperature range between 150 and 300°C, a 15 wt % loss occurs, associated to the decomposition of the UF shell. Moreover, a second marked degradation step involving the core material (60 wt %) is evident at higher temperatures. It is worth noting that the weight loss temperature of microencapsulated epoxy resin is higher than that of the bulk. This is due to the presence of homopolymerized species which formed during the heating process, as evidenced from DSC analysis (Fig. 5) and to the shielding effect of UF shell on the encapsulated, unreacted epoxy resin.

In the case of the samples C and E, that differ from the sample A on the reaction temperature and stirring rate used for their preparation (Table I) the same steps are detectable. However, the weight loss associated to the decomposition of epoxy resin portion are significantly reduced with respect to that observed in the case of sample A, while in the temperature range associated to the decomposition of the UF shell, a 28 wt % (sample C) and 54 wt % (sample E) loss occurs.

The small step observed at lower temperatures in the thermograms of samples C and E as well as in the case of neat UF could be ascribed to the decomposition of the UF oligomers.

These results are in agreement with the DSC data demonstrating that low reaction temperature and stirring rate lead not only to different low molecular weight UF species but also to a decreased encapsulation capability.

Moreover, TGA analysis has been used to asses the reliability of Raman spectroscopy as a quantitative analytical technique.

For this purpose, the weight loss associated to the degradation of UF shell has been taken into account to be used in the following equation:

$$\left(\frac{(\text{wt \%})\text{loss}_{\text{UF}}}{C_{\text{UF}}}\right)_{\text{neat}} = \left(\frac{(\text{wt \%})\text{loss}_{\text{UF}}}{C_{\text{UF}}}\right) \qquad (3)$$

where C_{UF} and (wt %) loss_{UF} refer, respectively, to UF concentration, expressed in weight %, and to the weight loss associated to the decomposition of UF shell. The subscripts *neat* refers to the sample composed by pure urea-formaldheyde, which has been used as reference.

By assuming a UF concentration equal to 100% in the neat UF, it was possible to determine the UF

TABLE III
Summary of Quantitative Analysis by Raman Spectroscopy

Sample	*I* (1722) (A.U.)	*I* (1585) (A.U.)	*I* (1722)/*I* (1585)	$W_{\text{epo}}/w_{\text{UF}}$	Epoxy resin (%)
Epoxy resin	–	93.5	–	–	100
Neat UF	21.34	–	–	–	0
A	15.22	96.09	0.16	2.72	73.1
B	13.5	72.6	0.19	2.32	70
C	23.95	80.21	0.3	1.43	59
D	8.65	6.94	1.25	0.34	25.6
E	11.84	3.68	3.22	0.13	11.8

concentration within each microcapsule sample. In particular, if we consider the case of sample A the percentage of UF, as evaluated from eq. (3), is 24 wt %. The amount of encapsulated epoxy resin, calculated as the complementary value to 100%, is 76 wt %.

The TGA results are in agreement with the Raman data confirming the reliability of this spectroscopic analysis as a quantitative analytical technique.

CONCLUSIONS

A series of UF/PY306 epoxy resin microcapsules has been prepared by *in situ* polymerization in an oil-in-water emulsion and the influence of reaction parameters on the microcapsule properties was described.

Morphological analysis showed for the samples A, B and C a complex morphology, characterized by the presence of micro-sized beads with a partially rough outer surface (single oil droplets), and/or clusters of nanocapsules. Irregularly shaped capsules (termed as *aggregates*) were also observed. In the case of samples D and E, obtained at lower reaction temperature and stirring rate, the morphology was different and characterized by a widespread amount of agglomerated nanosized particles.

DSC and TGA results indicated that a decrease of the reaction temperature, as well as of the stirring rate, has a great influence on the microcapsule properties. Low reaction temperature and stirring rate force the monomer to react in the aqueous rather than at the epoxy/water interface, leading not only to different chemical urea-formaldehyde derivatives but also to a decreased encapsulation capability.

FT-IR analysis demonstrated that no side reactions leading to the consumption of epoxy groups take place in the conditions used to prepare the microcapsules. In terms of the relative ratio of the two components in the microcapsules, the FTIR data qualitatively indicate that encapsulation has been successfully achieved for samples A and B. Sample C displays a roughly one-to-one ratio between the two components, whereas for sample D and even more so for sample E, the encapsulation procedure is to be considered inefficient.

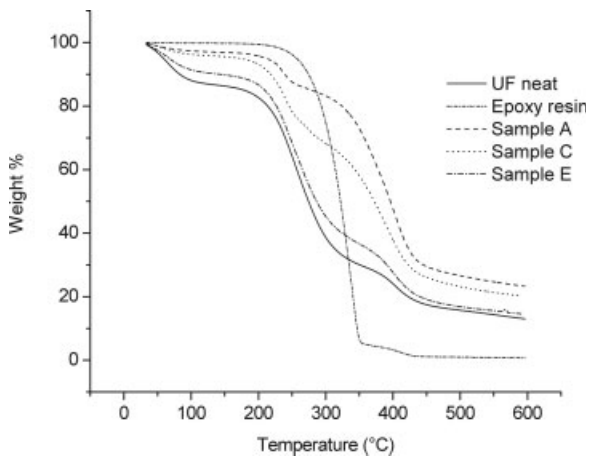

Figure 10 Thermogravimetric curves of analyzed samples.

TABLE IV
Thermal Properties of Epoxy Resin, Neat UF, and Microencapsulated Epoxy Resin

	I degradation step		II degradation step	
Sample	T_d[a] (°C)	Weight loss (%)	T_d[a] (°C)	Weight loss (%)
Epoxy resin			321	95.1
Neat UF	256	62	390	11
A	244	15	382	60
C	241	28	386	47.6
E	258	54	402	20

[a] The temperature when the weight loss percentage of the sample was 50 wt %.

A more precise analysis of the samples composition has been carried out by means of Raman spectroscopy. In particular, spectroscopic results confirmed that a decrease of the reaction temperature, as well as of the stirring rate, reduce the microencapsulability of the core material.

The main factor responsible for the epoxy resin microencapsulability seems to be related to the stirring rate. Most probably, the dispersion of the organic phase in the water, which is made progressively adverse by decreasing the reaction temperature, i.e., by passing from sample A to sample C, is further reduced by lowering the stirring rate, i.e. by passing from sample C to samples D and E. As a consequence of the low epoxy/water interfacial surface, the reaction between urea and formaldehyde occurs predominantly in the aqueous phase, according to the same mechanism proposed for the UF sample.

References

1. Tewes, F.; Boury, F.; Benoit, J. P. In Microencapsulation: Methods and Industrial Applications; Benita, S., Ed., Marcel Dekker: New York, 1996; p 1.
2. Sparks, R. E. In Encyclopedia of Chemistry and Technology, 3rd ed.; Grayson, M.; David, E., Eds.; Wiley: New York, 1981; Vol. 15, p 470.
3. Todd, R. D. Flavor Ind 1970, 1, 768.
4. Green, B. K.; Schleicher, L.U.S. Pat. 2,800,457 (1957).
5. Li, M.; Zhang, G. H.; Su, Z. G. J Chromatogr A 2002, 959, 113.
6. Tang, M.; Cao, X.; Liu, Z.; Wu, X.; Gance, D. Process Biochem 1999, 34, 857.
7. Russel-Jones, G. J. J Controlled Release 2002, 65, 49.
8. Uchida, T.; Shinosaki, K.; Nakada, Y.; Fukada, K.; Eda, Y.; Tokiyoshi, S.; Nagareya, N.; Matsuyama, K. Pharm Res 1998, 15, 1708.
9. Lintner, K.; Gabriele, D. E.U.S. Pat. 742,344 (2003).
10. Park, S. J.; Arshady, R. Microspheres Microcapsules Liposomes 2003, 6, 157.
11. Vaughn, L.; Whitaker, J. G.U.S. Pat. 744,243 (1996).

12. Gutcho, M. M. Microcapsules and Microencapsulation Techniques; Noyes Data: New Jersey, 1976.
13. Arshady, R. Microspheres, Microcapsules and Liposomes; Citrus Books: London, 1999.
14. Makino, K. Funtai Kogyo 1992, 24, 43.
15. Arshady, R. J Bioactive Compat Polym 1990, 5, 315.
16. Kondo, T. Pharm Tech Jpn 1991, 7, 263.
17. Hatate, Y.; Hamada, Y.; Nagata, H.; Imafuku, T. Kagaku Kogaku 1987, 51, 519.
18. Hatate, Y.; Yoshizawa, H. In The Polymeric Materials Encyclopedia: Synthesis, Properties and Applications; Salamone, J. C., Ed.; CRC Press: USA, 1996; Vol. 6, p 4341.
19. Yoshizawa, H.; Hatate, Y. Chem Eng 1993, 38, 405.
20. Yoshizawa, H.; Hatate, Y. Hyomen (Surface) 1995, 33, 552.
21. Takahashi, K.; Nozaki, S. IEEE Trans Compon Pack A 1995, 18, 245.
22. Taya, M. Compos A 1999, 30, 531.
23. Sheen, M. R.; MacBryde, J. C. Technovation 1995, 15, 99.
24. Ehrfeld, W. Electrochim Acta 2003, 48, 2857.
25. Manz, A.; Graber, N.; Widmer, H. M. Sens Actuat B 1990, 1, 244.
26. Zhang, X.; Tao, X.; Yick, K.; Wang, X. Colloid Polym Sci 2004, 282, 330.
27. White, S. R.; Sottos, N. R.; Geubelle, P. H.; Moore, J. S.; Kessler, M. R.; Spiram, S. R.; Brown, N. R.; Viswanathan, S. Nature 2001, 409, 794.
28. Dunky, M. Int J Adhes Adhes 1998, 18, 95.
29. May, C. A., Ed. Handbook of Epoxy Resins, Chemistry and Technology; Marcel Dekker: New York, 1988.
30. IUPAC Commission V. 4. Pure Appl Chem 1997, 69, 1451.
31. Marquardt, D. W. J Soc Ind Appl Math 1963, 11, 441.
32. Maddams, W. F. Appl Spectrosc 1980, 34, 245.
33. Meyer, B. Urea-Formaldehyde Resins. Addison-Wesley: MA, 1979.
34. Pizzi, A. In Wood Adhesives: Chemistry and Technology; Marcel Dekker: New York, 1983; p 59.
35. de Jong, J. I.; De Jonge, J. Rec TravChimPays-Bas 1952, 71, 643.
36. de Jong, J. I.; De Jonge, J.; Eden, E. A. K. Rec TravChimPays-Bas 1953, 72, 88.
37. Scopelitis, E.; Pizzi, A. J Appl Polym Sci 1993, 48, 2135.
38. Brown, E. N.; Kessler, M. R.; Sottos, N. R.; White, S. R. J Microencapsul 2003, 20, 719.
39. Galia, M.; Mantecon, A.; Ca'diz, V.; Serra, A. Makromol Chem 1990, 191, 1111.
40. Wang, M. S.; Pinnavaia, T. J Chem Mater 1994, 6, 468.
41. Edwards, H. G. M. In Handbook of Vibrational Spectroscopy; Chalmers, J. M.; Griffiths, P. E., Eds.; Wiley: New York, 2002; Vol. 3, p 1838.
42. Hill, C.; Hedren, A. M.; Myers, G.; Koutsky, J. A. J Appl Polym Sci 1984, 29, 2749.
43. Rocks, J.; Rintoul, L.; Vohwinkel, F.; George, G. Polymer 2004, 45, 6799.